# Non-Subsampled Contourlet Transform based Multimodal Medical Image Fusion and its Performance Evaluation

**Shaik Afroz Begum, K.Suresh Reddy, M.N.Giri Prasad**

***Abstract*— Integration of medical images from different sensors can create data that can't be obtained by observing the images separately. Here, in this framework, the fusion of the images is implemented using non-subsampled Contourlet transform (NSCT) and this tool offers some special features like multi-resolution, invariant shifting, and multi-directional band decomposition tool. First, the input images of medical field decomposed into complementary low frequency and frequency of high range sub-bands by NSCT is implemented. Then, by considering the significance of these complementary sub images, a new selection method is implemented in different ways. This scheme use local energy rule to select the low-frequency band and the weighted sum of modified Laplacian (WSML) rule to select high-frequency directional bands. In the final step, the merged image is recovered by inverse NSCT tool implementation on merged bands. This effective novel fusion scheme is compared with existing traditional image merging rules in the transform domain. The results can reveal the efficiency of the novel fusion structure through visual and quantitative measures.***

***Keywords*— Nonsubsampled contourlet transform, Computed Tomography(CT) image, Magnetic resonance Imaging(MRI), Local energy, Modified Laplacian.***

## 1. INTRODUCTION

Emergence in extensive number of medical instruments like: CT sensor, MRI sensor, X-ray, ECG, and so forth have been included in visual output of these sensors regarding analysis and clinical investigation [1-3]. In medical field, the doctor can detect diseases accurately by extracting and analyzing sufficient data from the medical sensors. The acquired images of various sensors contain complementary data, i.e., a sensor images lack the details of another imaging sensor. For instance, a CT image contains the details of bony structure, and MRI represents the soft tissue information. Hence, a doctor always prefers to do the simultaneous investigation of the output of multi-medical modalities. Through image integration (fusion) techniques, there is a possibility to merge multiple images and present significant information in an effective way [4-5]. Fused medical images present more and significant information to Neurologists, Oncologists, Cardiologists, and others. In current years, a series of fusion algorithms have been developed. The existing fusion algorithms are categorized into multi-modal, multi-focus, multi-view and multi-temporal techniques.

**Revised Manuscript Received on March 10, 2019.**

**Shaik Afroz Begum,** Research Scholar, ECE Department, JNTUA, Andhra Pradesh, India.(Email:afroz.phd16@gmail.com)

**Dr.K. Suresh Reddy,** Professor & Head, ECE Department, G Pulla Reddy Engineering College, Andhra Pradesh, (India. Email:sureshkatam@gmail.com)

**Dr.M.N. Giri Prasad,** Professor, ECE Department, JNTUA, Andhra Pradesh, India. (Email:giriprasadmn@jntua.ac.in)

Presently, the merging rules of images are preferred to implement by multi-scale decomposition (MSD) technique. The biomedical images are separated into high-frequency (HF) and low-frequency (LF) sub-bands, and these bands are merged via different fusion rules in transform domain. In the final step, implementing the inverse MSD of the merged coefficients to recover the image in spatial domain. The quality of any fused image relies on the selection of the domain and merging rules. The general procedure of merging in transform domain is as shown in Fig 1.

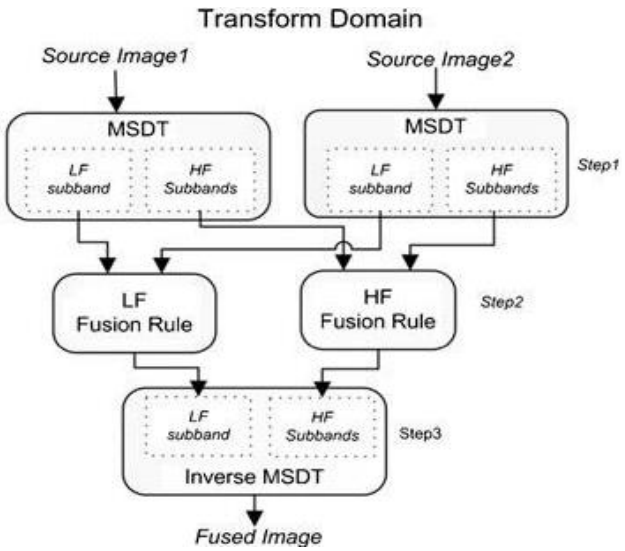


**Fig.1.Tansform domain Image fusion**

The Contourlet transform (CT) is used to represent the images in real two-dimensional transform domain space [6]. Here, the Laplacian pyramid (LP) is decomposing the source medical images in to various bands [7], and after that the directional filters are applied to distinct the coefficients of sub-bands to understand the anisotropic properties. The decomposition of images into multi-scales and multi-direction sub-bands is possible with the CT tool. The pseudo-Gibbs phenomenon is observed at image singularities due to shift invariant property of CT. NSCT[8] has been proposed in 2006 and this is effectively applied to reduce image noise, enhancement of images, and integrating images etc. NSCT acquired the perfect qualities of CT as well as it offers the characteristics of shift-invariance, better directionality, and regularity. To include all important features in this fusion work, NSCT is selected to transform an image in to multiple bands.

The work presented in this framework is organized in the following sections: II section explains an image decomposition procedure in NSCT domain and III section illustrates fusion rules of medical images. The results of simulation work and its quantitative measures will be observed in Section IV. Lastly, the section V concludes the proposed work.

## II. NON-SUBSAMPLED CONTOURLET TRANSFORM

NSCT tool offers multi-directional feature, shift-invariant feature, and multi-resolution feature [8-11]. It is implemented by combining the non-subsampled directional filter bank (NSDFB) and non-subsampled pyramid structure (NSP). NSP offers the feature of multiscale and the multi-direction feature is provided by NSDFB. The important Shift-invariance feature of NSCT is achieved by avoiding downsampling and upsampling processes in NSDFB and NSP as well. The NSCT is implemented through the combination of the NSP and NSDFB as shown in below Fig.2a and Fig. 2b.

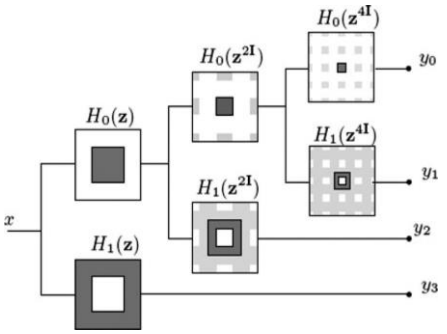


**Fig.2a. Multi-stage decomposition using NSP.**

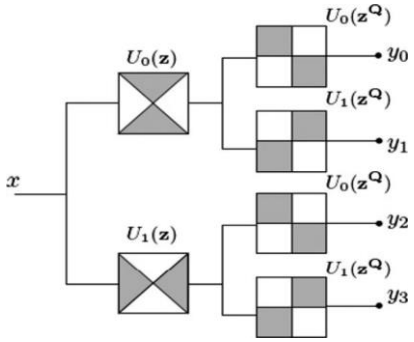


**Fig.2b. Directional bands generation using multi-channel NSDFB.**

### A. NSP

The NSP has a two-channel filter bank block without down samplers and upsamplers. Each level of NSP generates one low-pass sub-image (y0) and one bandpass sub-image (y1). The three-level decomposition using NSP is presented in Fig. 2a. The NSP filter banks of the following stages are executed via upsampling the previous stage filters. The above feature of NSCT eliminates the requirement of additional channel. The initial level LF and HF filters are signified as H0(Z) and H1(Z) respectively and next level LF and HF filters are given by H0(Z2) and H1(Z2), respectively.

### B. NSDFB

The bandpass images of NSP are entered NSDFB to obtain directional bands. The NSDFB consists of a two-channel fan filter bank as its basic structure which is presented in Fig. 2b. The analysis filters are given as Um(Z) (m =0,1) and synthesis filters are given as Vm(Z) (m =0,1).

## III. PROPOSED METHOD

The multi-modality images (MRI and CT) are considered and these images comprises of significant and complementary information. For precise detection and fast diagnosis, all these details must be extracted into a single highly informative image. In this fusion work, the NSCT has been applied to integrate the brain images. The initial step of the novel fusion algorithm is to change the considered bio-medical images into LF sub-band images and HF directional sub-band sets of different scales. These multi-scale image sets are then merged utilizing individual fusion rules [12-13].

### A. LF Sub-Band Fusion of last decomposition level

Low-frequency sub-bands of medicinal images are approximated forms of the original image. In this work, the NSCT decomposition levels have been confined to two, therefore the LF band has most of the image energy and last level of decomposition contains few high frequency details. Consequently, the low-frequency sub-band images are merged for preserving approximate information as well as details present in it. The fusion rule in this work applied to LF bands is the local energy of the coefficients in a 3×3 window. The activity of LF coefficient CAL(x,y) of the image A at position (x, y) obtained using the following expression.

$$e_A(x,y) = \sum_{x=-1}^{x=1}\sum_{y=-1}^{y=1}\left(C_A^L(x,\ y)\right)^2 \qquad (1)$$

Similarly, the image B local energy of the low-frequency coefficient CBL(x,y) at location (x, y) is:

$$e_B(x,y) = \sum_{x=-1}^{x=1}\sum_{y=-1}^{y=1}\left(C_B^L(x,\ y)\right)^2 \qquad (2)$$

The initial image fusion decision map (DL(x,y)) of merged coefficients(images) is obtained by selecting the sub-band coefficient with the maximum activity i.e. if (DL(x,y)) = 1 then the coefficient of image A is selected at (x, y) location and if (DL(x,y)) = 0 then image B coefficient is selected. Then, by using a majority filter, consistency verification is done in a 3×3 window to obtain final image fusion binary decision map (Df). Therefore, in each 3×3 region, the condition where most coefficients observed from image A and only the center coefficient is derived from image B, therefore for such cases, the center coefficient also have to be taken from the image A. Otherwise, the coefficient value will remain same. This verification process gets repeated at each coefficient of fused low-pass sub-band. The neighboring coefficients are considered in this process

to eliminate the noise problem and therefore ensure the presence of homogeneity feature in the fused image.

### B. HF directional Sub-Bands Fusion Rule

HF (directional) sub-bands provide various features of the source image, which includes: contours, edges, boundaries and lines, etc. High frequency bands use the conventional fusion rules to select the coefficient that achieves maximum absolute value. This process is highly sensitive to noise pixels and there is a chance of losing some important information when selection is according to a single coefficient rather than the neighboring coefficients. The effective fusion rule for activity level measurement which preserves fine details of the image in all directions is considered and it integrates the HF coefficients without introducing noise. While dealing with our proposed work, the weighted sum of modified Laplacian (WSML) fusion scheme is employed on HF sub-band coefficients as a activity measure.

Modified Laplacian is applied to I(x,y) and is specified by expression (3).

$$ML_I = \left|2*I(x,y)-I(x-1,y)-I(x+1,y)\right| + \left|2*I(x,y)-I(x,y-1)-I(x,y+1)\right| \quad (3)$$

WSML of $I$(x,y) is given by the equation (4),

$$WSML_I(x,y) = \sum_{m=-1}^{1}\sum_{n=-1}^{1}(w(m+1,n+1))*(ML_I(x+m,y+n)) \quad (4)$$

Here w is the matrix which contains weights for HF rule implementation. The city block distance measure is proposed for the calculation of weight matrix in our proposed work and it is given as,

$$w = \frac{1}{16}\begin{bmatrix}1 & 2 & 1\\ 2 & 4 & 2\\ 1 & 2 & 1\end{bmatrix}$$

On each HF(directional) coefficients CAij, and CBij of A and B images, WSML is calculated. Here, CAij is ith decomposition level, jth directional HF band coefficient of the image A and CBij is ith level, jth directional HF band coefficient of image B having their position as (x,y) with their activity measure.

WSML expression is computed at each HF(directional) sub-band coefficient CAij, and CBij of images at location (x,y) as their activity measure. Thus at the end, a final binary decision map (Df) is found by means of consistency verification which is considered in the low-frequency scheme.

Finally, the spatial domain fused image is recovered by the implementation of two-level inverse NSCT on merged coefficients.

## IV. EXPERIMENTAL RESULTS AND PERFORMANCE EVALUATIONS

The investigations on an effective image fusion scheme have been made with two different data sets of brain images. Dataset-1 and dataset-2 contains CT and MRI (multi-modal images) images (shown in Fig. 3a, b and Fig. 4a, b) corresponding to various pathologies. This novel fusion scheme is compared with existing transform based image fusion techniques like (i)DWT [14-16], (ii)SWT [17] (iii)CT [6], and (iv)NSCT [8] image fusion methodologies using basic merging rule, i.e. by analyzing the absolute maximum value for HF directional bands and the averaging process is done for LF frequency sub-band. They include: (i) DWT_av_mx, (ii)SWT_av_mx (iii)CT_av_mx, and (iv) NSCT_av_mx. Simulation results are shown in Figs. 3 and 4.

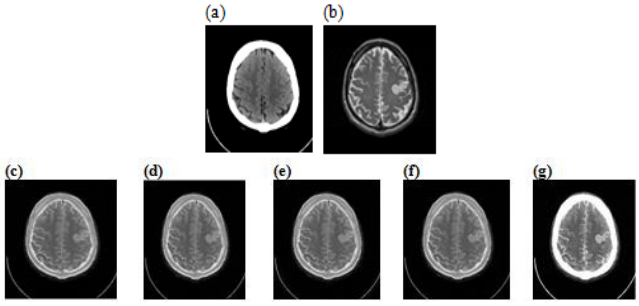


**Fig. 3 Comparison of various transform domain fusion methodologies with brain (Dataset-1)images. (a) CT Sensor output (b) MR Sensor output (c) DWT(av_mx) (d) SWT(av_mx) (e)CT(av_mx) (f) NSCT(av_mx) (g) Proposed method**

Visual analysis of the experimental results show that the proposed fusion rules retain the fused MRI as well as CT images with better contrast, showing clear hard and soft tissue information without any artifacts.

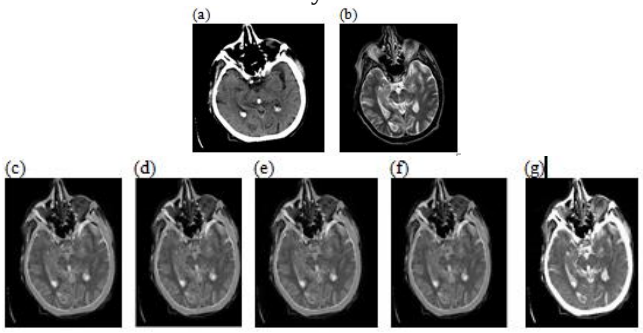


**Fig. 4 Comparison of various transform domain fusion techniques for brain (Dataset-2) images. (a)CT Sensor ouput (b)MRI Sensor output (c) DWT(av_mx) (d) SWT(av_mx) (e)CT(av_mx) (f) NSCT(av_mx) (g) Proposed method**

The performance of this work is evaluated with quality measurement metrics like (1) Mutual Information(MInf), (2) Information Entropy(En), (3) Spatial Frequency(SFr), (4) Ratio of spatial frequency error(RSFErr), (5) Correlation coefficient(CorC)

1. MInf: Mutual info represents the details that one sensor image comprises of other sensor image details. Assuming sensor images A and B, in addition to that an integrated image (F), the quantity of data that image(F) encompasses about A and B is considered as:

$$MI_{FA}= \sum_{F,A} P(F,A)\log\frac{P(F,A)}{P(F)P(A)} \quad (5)$$

$$MI_{FB}= \sum_{F,B} P_{FB}(F,B)\log\frac{P(F,B)}{P(F)P(B)} \quad (6)$$

Thus the Mutual information is computed as

$$MI_F = MI_{FA}+MI_{FB} \quad (7)$$

2. En: Information entropy computes the quantity of data existing in images. Higher entropy denotes the more data capacity. According to the Shannon data philosophy, the IE of a fused image is specified by the mathematical expression.

$$En = -\sum_{k=0}^{L-1} P_F(k)\log_2 P_F(k) \quad (8)$$

3. SFr: The Spatial Frequency measures the activity level of image(F) and it tells about amount of fine details.

$$SFr= \sqrt{R_F^{\,2}+C_F^{\,2}} \quad (9)$$

Here, $R_F$ : The row frequency and
$C_F$ : The column frequency.
An image with a large spatial frequency will have better fusion quality.

4. RSFErr: The Spatial frequency error reveals the differences amid the activity of fused image as well as the reference ideal fused image, which is expressed as follows:

$$RSFErr = (SFr_F - SFr_R)/SFr_R \quad (10)$$

Here SFrF is said to be the fused image spatial frequency and SFrR is referred as the reference ideal image spatial frequency.

5. CorC: Correlation coefficient measures similarity of small objects present in the input and fused images. Higher the value of correlation, more the information preserved in the image(F). CorC between image IA and the fused image IF is expressed as:

CorC(IF,IA)=

$$\frac{\sum_{x=0}^{M-1}\sum_{y=0}^{N-1}(I_F(x,y)-\overline{I_F})(I_A(x,y)-\overline{I_A})}{\sqrt{\sum_{x=0}^{M-1}\sum_{y=0}^{N-1}(I_F(x,y)-\overline{I_F})^2\sum_{x=0}^{M-1}\sum_{y=0}^{N-1}(I_B(x,y)-\overline{I_B})^2}} \quad (11)$$

Here, the quantity $\overline{I_F}$ as well as $\overline{I_A}$ are considered as the average values of the F and A images. Repeat the above expression to compute CorC($I_F$,$I_B$).

Tables I and II show the quality measurement metrics of integrated fused images for two pairs of medical images. The best values are highlighted for each quality metric in Tables I and II. The advantages of effective NSCT scheme over other existing methods are shown in visual analysis results and furthermore they are reliable with the quality metrics. Henceforth, the novel merging rules in NSCT domain are appropriate for MRI-CT image merging.

**TABLE I Evaluation of quality metrics for Fused Medical Images(Dataset-1) (Shown In Fig. 3a, b)**

| Fusion method | Metrics | | | | | |
|---|---|---|---|---|---|---|
| | ***IE*** | ***MI*** | ***SF*** | ***RSFE*** | ***CC1*** | ***CC2*** |
| DWT_average_max | 5.5471 | 3.0699 | 27.2902 | -0.1401 | 0.8711 | 0.7248 |
| SWT_average_max | 5.4616 | 3.2492 | 23.4849 | -0.2710 | 0.8772 | 0.7303 |
| CT_average_max | 6.2897 | 2.9314 | 28.4287 | -0.1515 | 0.8714 | 0.7253 |
| NSCT_average_max | 5.3717 | 3.4119 | 22.2680 | -0.2953 | 0.8790 | 0.7315 |
| **Proposed** | 5.7532 | **3.7998** | **36.9700** | **0.1608** | **0.9044** | 0.6082 |

**TABLE II Evaluation of quality metrics for Fused Medical Images( Dataset-2) (Shown In Fig. 4a, b)**

| Fusion method | Metrics | | | | | |
|---|---|---|---|---|---|---|
| | ***IE*** | ***MI*** | ***SF*** | ***RSFE*** | ***CC1*** | ***CC2*** |
| DWT_average_max | 5.3739 | 3.5774 | 22.6149 | -0.1380 | 0.9278 | 0.8283 |
| SWT_average_max | 5.2767 | 3.8620 | 19.8283 | -0.2592 | 0.9308 | 0.8314 |
| CT_average_max | 5.9242 | 3.2381 | 23.4822 | -0.1479 | 0.9277 | 0.8285 |
| NSCT_average_max | 5.2213 | 4.0523 | 18.1489 | -0.2992 | 0.9319 | 0.8325 |
| **Proposed** | 5.7014 | **4.5622** | **30.2424** | **0.1374** | **0.9595** | 0.7146 |

## V. CONCLUSION

An effective Multi-modal image fusion in NSCT domain has been proposed to integrate biomedical images. In this fusion work, the datasets of CT and MRI images have been combined through two individual fusion schemes to preserve the more information present in multi-directional bands. The LF bands are integrated by considering local energy rule, whereas weighted sum-modified Laplacian is considered as the HF fusion rule. In our work, two data sets of brain images including CT and MRI images are integrated using traditional fusion techniques and the proposed image fusion. The visual and quantitative measures clearly explain that the proposed fusion framework can retain more details of images (CT and MRI) with enhancement of details and less distortion than conventional fusion methods.


*Published By:*
*Blue Eyes Intelligence Engineering*
*& Sciences Publication*

## REFERENCES


1. B.S. Hoyle, “A schema for generic process tomography sensors,” IEEE Sensors J., vol. 5, no. 2, pp. 117–124, Apr. 2005.
2. A.Alkan, S.A.Tuncer, and M.Gunay, ‘‘Comparative MR image Analysis for thyroid nodule detection and quantification,’’ Measurement, vol.47, pp. 861-868, Jan. 2014.
3. Alex Pappachen James, Belur V. Dasarathy: ‘‘Medical image fusion: A survey of the state of the art’’, Information Fusion 19 (2014) 4–19, Volume 19, Sep 2014, pp 4-19, Elsevier.
4. Zaid Omer and Tania Stathaki,"Image fusion: An overview" in fifth International conference on Intelligent systems, Modelling and Simulation, IEEE 2014.
5. Gemma Piella,: Image Fusion for Enhanced Visualization:A Variational Approach International journal on Computer Vision, Volume 83, Issue 1,June 2009,pp 1-11
6. M.N.Do and M. Vetterli, “The contourlet transform: An efficient directional multiresolution image representation,” IEEE transactions on Image processing, Volume 14, Issue 12, Dec 2005,pp. 2091-2106.
7. Burt, P.T., Anderson, E.H., 1983. The Laplacian pyramid as a compact image code. IEEE Trans. Comm. 31, 532–540.
8. Arthur L. da Cunha, Jianping Zhou, Member, IEEE, and Minh N. Do, Member, ‘‘The Nonsubsampled Contourlet Transform: Theory, Design, and Applications’’, IEEE Transactions On Image Processing, Vol. 15, No. 10, October 2006
9. Yang, L., Guo, B.L., Ni, W.: Multimodality medical image fusion based on multiscale geometric analysis of contourlet transform, Neurocomputing, Volume 72, Issues (1–3), Dec 2008, pp 203–211.
10. Vikrant Bhateja, Himanshi Patel, Abhinav Krishna, Akanksha Sahu, and Aimé Lay- Ekuakille: Multimodal Medical Image Sensor Fusion Framework Using Cascade of Wavelet and Contourlet Transform Domains,IEEE Sensors Journal, Volume 15, Issue. 12, Dec 2015,pp 6783-6790
11. Gaurav Bhatnagar, Q.M. Jonathan W, and Zheng Liu,: “Directive Contrast Based Multimodal Medical Image Fusion in NSCT Domain, IEEE Transactions on Multimedia, volume 15, Issue 5, Aug 2013,pp.1014-1024.
12. Richa Srivastava, Om Prakash, Ashish Khare,“Local energy-based multimodal medical image fusion in curvelet domain," IET Computer Vision, Volume 10, Issue 6, Sep 2016, pp 513-527.
13. P Ganasala and V Kumar, ‘‘CT and MR image fusion scheme in NSCT domain’’ in Journal of digital imaging 27 (3), 407-418, 2014, Springer.
14. Gonzalo Pajares and Jesus Manuel de la Cruz, “ A wavelet-based Image Fusion Tutorial” in Pattern Recognition, Volume 37, Issue 9, Sep 2004, pp. 1855-1872, Elsevier.
15. Hui Li, B.S.Manjunath, and Sanjit K.Mitra, " Multi-sensor Image fusion using the wavelet transform" in Image Processing, 1994. Proceedings. ICIP-94., IEEE International Conference.
16. Vijayarajan R, Multan S, “ Discrete wavelet transform based Principal component averaging fusion for medical images’’, AEU - International journal of electronics and Communications, Volume 69, Issue 6, June 2015, pp 896–902, Elsevier.
17. Mirajkar Pradnya P and Sachin D.Ruikar, “Image fusion based on Stationary wavelet transform” in International Journal of Advance research and studies,2013.
18. Zheng Y, Essock E A, Hansen BC, Haun AM, ‘‘A new metric based on extended spatial frequency and its application to DWT based fusion algorithms" in Information Fusion, Vol 8, pp 177-192,2007.
19. Qu G, Zhang D,Yan P, ‘‘ Information measure for performance of image fusion’’, Electronic Letters,38,pp 313-315,2002.



Published By:
Blue Eyes Intelligence Engineering
& Sciences Publication